Check for updates

Defective hematopoiesis and hepatic steatosis in mice with combined deficiencies of the genes encoding Fancc and Cu/Zn superoxide dismutase

Suzana Hadjur, Karen Ung, Louis Wadsworth, James Dimmick, Evica Rajcan-Separovic, Richard W. Scott, Manuel Buchwald, and Frank R. Jirik

Several lines of evidence point to an abnormality in the response of Fanconi anemia cells to reactive oxygen species. To investigate the potential pathologic consequences of an in vivo alteration of redox state in mice lacking one of the Fanconi anemia genes, animals were generated having combined deficiencies of the cytosolic Cu/Zn superoxide dismutase (*Sod1*) and Fanconi anemia complementation group C (*Fancc*) genes. Interestingly, hepatocytes of *Fancc*$^{-/-}$*Sod1*$^{-/-}$ mice exhibited a zonal pattern of microvesicular steatosis, possibly as a result of oxidative stress-induced injury to hepatocyte membranes. Consistent with this idea, freshly explanted *Fancc*$^{-/-}$*Sod1*$^{-/-}$ hepatocytes demonstrated increased spontaneous production of superoxide in vitro. The second phenotypic feature of *Fancc*$^{-/-}$ *Sod1*$^{-/-}$ mice was that of bone marrow hypocellularity accompanied by significant decreases in peripheral blood erythrocyte and leukocyte numbers as compared with wild-type controls. Although flow cytometry analysis with monoclonal antibodies against cell surface antigens revealed normal numbers of primitive hematopoietic progenitor populations in *Fancc*$^{-/-}$*Sod1*$^{-/-}$ marrow, lineage-positive progenitor numbers were significantly reduced in these mice. Furthermore, the in vitro clonogenic growth of *Fancc*$^{-/-}$*Sod1*$^{-/-}$ erythroid, myeloid, and early B-lymphoid colonies in semisolid media was profoundly compromised. These results suggested that the altered redox state likely present in *Fancc*$^{-/-}$ *Sod1*$^{-/-}$ hematopoietic progenitors was responsible for an impairment of cell proliferation or survival. (Blood. 2001;98: 1003-1011)

© 2001 by The American Society of Hematology

Introduction

Fanconi anemia (FA) is an autosomal recessive disease of childhood characterized by progressive pancytopenia, various developmental abnormalities, and a predisposition to acute myeloid leukemia.[1] Most individuals with FA, however, succumb to the complications of aplastic anemia.[2] FA cells demonstrate increased sensitivity to DNA cross-linking agents such as mitomycin C (MMC), diepoxybutane, and cisplatin,[2,3] a feature that serves as the basis for an important diagnostic test. FA cells treated with these cross-linking agents show a striking increase in double-strand DNA breaks and inhibited growth with cell cycle arrest in G_2.[2] To date at least 7 potential FA genes have been indicated by complementation studies, and most of these genes, *FANCA*, *FANCC*, *FANCD2*, *FANCE*, *FANCF*, and *FANCG*, whose mutations account for 6 of the complementation groups, have now been characterized.[4-10] Despite the variety of genes involved in this disorder, mutations in *FANCA* and *FANCC* account for approximately 80% of all patients with FA.[11] Murine *Fancc*, being highly similar to the human ortholog, is able to complement human cells deficient in *FANCC*, restoring MMC resistance.[12] *Fancc*-deficient mouse strains were generated through gene targeting. Both had similar phenotypes,[13,14] demonstrating compromised gametogenesis, and an increase in the number of chromosomal aberrations, both spontaneously and after exposure to MMC. However, the targeted lines recapitulated neither the developmental nor the hematologic defects typical of human FA.[13,14] The reason for this interspecies discordance is unknown, but it has limited the utility of the mutant mice as potential models of FA.

A number of hypotheses regarding the nature of the primary defect in FA have been suggested, including the proposal that FA proteins constitute a DNA damage recognition and signaling pathway, whose impairment is manifested by chromosomal instability and increased sensitivity to interstrand DNA cross-linking agents.[15] Although a reduced ability to process DNA cross-links is clearly evident, it has also been proposed that an abnormal reduction of MMC in FA cells leads to the production of reactive species that in turn generate cross-links and other types of oxidative lesions.[16] Thus, FA might also result, at least in part, from an abnormal regulation of cell redox state or of the cellular response to oxidative stress or both. In support of this notion, addition of Cu/Zn superoxide dimutase (SOD) to the culture medium of FA cells was reported to attenuate chromosomal breakage as well as MMC cytotoxicity,[16] an effect also observed in FA cells overexpressing thioredoxin.[17] In keeping with an inability to regulate either production, or the consequences of reactive oxygen species (ROS), some FA cells were shown to be hypersensitive to oxygen.[16,18] Thus, cells grew slowly at elevated oxygen levels (eg, 35%) and

From the Centre for Molecular Medicine and Therapeutics, and the Departments of Medicine and Pathology, British Columbia Research Institute for Children's and Women's Health, University of British Columbia, Vancouver, British Columbia, Canada; Cephalon Incorporated, West Chester, Pennsylvania; and Genetics and Genome Biology, Hospital for Sick Children, Toronto, Ontario, Canada.

Submitted October 3, 2000; accepted April 19, 2001.

Supported by grants no. 010265 (to F.R.J.) and 007223 (to M.B.) from the National Cancer Institute of Canada, with funds from the Canadian Cancer Society. S.H. was supported by a Studentship from the Cancer Research Society of Canada.

Reprints: Frank R. Jirik, Department of Biochemistry and Molecular Biology, University of Calgary, 3330 Hospital Dr NW, Calgary, Alberta, T2N 4N1 Canada; e-mail: jirik@ucalgary.ca.

The publication costs of this article were defrayed in part by page charge payment. Therefore, and solely to indicate this fact, this article is hereby marked "advertisement" in accordance with 18 U.S.C. section 1734.

© 2001 by The American Society of Hematology

Downloaded from http://ashpublications.net/blood/article-pdf/98/4/1003/1676353/h8160101003.pdf by guest on 05 June 2024

tended to arrest at G_2, whereas at low oxygen concentrations (eg, 5%) growth was normal and accompanied by decreased chromosomal aberrations.[18-20] Increased production of ROS by FA cells, such as leukocytes and fibroblasts, has also been reported, suggesting that FANCC might regulate the generation of these species.[21,22] A potential endogenous source of superoxide, the NADPH cytochrome P-450 reductase (RED) system, has also been implicated in FA. Not only were chromosomal breaks in FA cells reduced by cytochrome P-450 inhibition, but evidence of a direct physical interaction between FANCC and RED was reported,[23,24] leading to the hypothesis that FANCC might protect cells from ROS via regulation of RED activity.

Mice with a targeted disruption of the gene encoding the cytosolic Cu/Zn SOD (*Sod1*) exhibit normal growth and development; however, they show a distinctive motor axonopathy[25,26] and impaired gametogenesis.[27] The limited spontaneous pathology of *Sod1*$^{-/-}$ mice suggested that although this enzyme might function to modulate superoxide-mediated effects in some tissues under basal conditions, that it was of critical importance during exposures to specific pro-oxidant stimuli.[28,29] In keeping with this, *Sod1*$^{-/-}$ embryonic fibroblasts exposed to the superoxide-generating herbicide, paraquat, were much more sensitive than wild-type cells.[30]

We hypothesized that a lack of *Sod1* might reveal a role for alterations in redox state with respect to the development of a FA-like syndrome in *Fancc*-deficient mice. To examine this possibility, we generated mice with combined deficiencies of both the *Fancc* and *Sod1* genes. Interestingly, *Fancc*$^{-/-}$*Sod1*$^{-/-}$ mice developed liver pathology as well as bone marrow (BM) hypocellularity and peripheral blood (PB) bicytopenia (erythrocytes and leukocytes), accompanied by a profound reduction of the clonogenic growth of hematopoietic precursors in vitro.

Materials and methods

Generation of *Fancc*$^{-/-}$*Sod1*$^{-/-}$ mice and histologic analysis

Fancc$^{+/-}$ mice[14] were crossed with *Sod1*$^{+/-}$ mice[28] to obtain mice that were heterozygous at both loci. Locus-specific polymerase chain reaction (PCR) was used to genotype mice. Brother-sister matings of *Fancc*$^{+/-}$*Sod1*$^{+/-}$mice were carried out to produce litters having *Fancc*$^{-/-}$ *Sod1*$^{-/-}$ mice. Mice, 8 to 10 weeks of age, were of a mixed genetic background and thus littermate controls were used in all experiments. Viral antibody-free mice were housed in the Center for Molecular Medicine and Therapeutics barrier facility according to protocols approved by the Animal Care Committee at the University of British Columbia. For light microscopy, tissue samples were either frozen or fixed in 4% paraformaldehyde solution and embedded in paraffin and bone sections were first decalcified before processing. For paraffin-embedded sections, hematoxylin and eosin, periodic acid-Schiff with and without diastase, and Masson trichrome were used. Frozen sections were stained with oil-red-O. For electron microscopy, liver blocks were fixed in cold 3% gluteraldehyde and stored at 4°C. Samples were rinsed twice in Millonig buffer (pH 7.4) and were subsequently fixed in 1% osmium tetroxide in Palade solution for 1.5 hours at 4°C. Samples were stained en bloc for 15 minutes with 2% aqueous uranyl acetate and then dehydrated before embedding. Sections were examined with a Phillips 400 electron microscope.

Blood collection, serum alanine aminotransferase measurement, and PB counts

Following Avertin overdose, blood was obtained by cardiac puncture, and either allowed to clot at room temperature, or added to microtainer tubes, pretreated with EDTA, for blood counts. Clotted blood was centrifuged at 14 000 rpm for 5 minutes, and serum was removed and frozen at −80°C. Serum alanine aminotransferase (ALT) levels were determined using a Beckman Synchron CX7. PB counts were performed using a Sysmex 9500 analyzer. Red blood cell (RBC), white blood cell (WBC), platelet, hemoglobin, and mean cell volume (MCV) values were determined.

Tissue isolation

Mice were killed at 8 to 10 weeks of age by intraperitoneal injection of 4% Avertin (0.01 mL/g). Samples were harvested from the same region of the liver in all mice. Single-cell suspensions were prepared by pressing samples through a wire mesh into cold serum-free RPMI 1640 (Life Technologies, Burlington, Ontario, Canada). Cells were then passed through a 40-μ nylon filter to remove clumps and debris. Liver cells were pelleted at 1500 rpm and resuspended in cold RPMI. Total BM cells were collected by flushing femurs from 7- to 8-week old mice with cold Hanks balanced saline solution with 5% fetal calf serum (FCS). Cell viability, more than 90% in all samples, was determined by trypan blue exclusion.

Superoxide quantitation

Isolated liver cells were resuspended, in triplicate, at a density of 5.0×10^5/mL in serum-free RPMI and centrifuged at 1500 rpm, before being resuspended in 100 μL Superoxide Assay Medium (Calbiochem, San Diego, CA). Each culture was then placed into a well of an opaque 96-well polystyrene flat-bottomed microtiter plate (VWR Canlab, Mississauga, Ontario, Canada) kept on ice until analysis. Then, 5.0 μL 4.0 mM luminol solution (Calbiochem), diluted in 95 μL Superoxide Assay Medium, was added simultaneously to all samples. Chemiluminescence was measured at 1 minute after luminol addition using a MLX Microtiter Plate Luminometer (Dynex Technologies, Chantilly, VA). The average intensity of the triplicates was recorded as relative light units (RLUs). Purified SOD (Calbiochem) was added to the cells as a specificity control to show that chemiluminescence was due to superoxide.

Immunoblotting and densitometry

Flash-frozen liver samples were lysed in Nonidet P-40 lysis buffer (1% Nonidet P-40, 150 mM NaCl, 50 mM Tris, pH 7.5, and 10% glycerol) in the presence of multiple protease inhibitors (Boehringer Mannheim, Indianapolis, IN and BDH, Toronto, ON). Lysates were centrifuged for 15 minutes at 14 000 rpm. Liver protein concentration was determined by an assay based on the Bradford method. Lysate volume corresponding to 250 μg total protein was diluted 3:1 with Laemmli sample buffer. Samples were boiled for 5 minutes before electrophoresis. Total cell lysates were separated by sodium dodecyl sulfate–polyacrylamide gel electrophoresis (SDS-PAGE) at 150 V and transferred to nitrocellulose paper by electroblotting at 100 V for 1 hour at room temperature in a solution containing 192 mM glycine, 25 mM Tris, and 20% methanol. Filters were blocked overnight at 4°C in TBST (10 mM Tris, pH 8.0, 150 mM NaCl, and 0.05% Tween-20) containing 5% bovine serum albumin (BSA). Filters were then incubated for 60 minutes at room temperature in TBST with 1% BSA with one of the following antibodies (Stressgen Biotechnologies, Victoria, BC): anti-MnSOD (1:5000), HO-1 (1:2000), or anti–β-tubulin (1:250). After 3 TBST washes, filters were incubated for 1 hour with a horseradish peroxidase–conjugated secondary antibody (Dako Diagnostics, Mississauga, ON). Proteins were detected by chemiluminescence (Amersham, Arlington Heights, IL) using Biomax MR film (Eastman Kodak, Rochester, NY). Densitometry was performed using a GS300 reader (Hoefer Scientific Instruments, San Francisco, CA), and results were analyzed using the GS370 1-D Data System, version 2.0 for Macintosh.

Flow cytometry

A total of 1×10^6 cells was resuspended in 500 μL phosphate-buffered saline (PBS) plus 2% FCS (FACS buffer), blocked on ice with 1 μg anti-FcγRIIb (2.4G2, Pharmingen, Mississauga, ON) for 20 minutes, and then stained with either 0.5 μg anti-CD11b–fluorescein isothiocyanate (FITC; for liver samples) or one of the following FITC-conjugated antibodies for 30 minutes on ice (BM cells): PGP1, B220, Ly6G (Gr-1), 7-4 CD11b, CD14 and TER-119; and (primitive populations): Sca1, c-kit,

Downloaded from http://ashpublications.net/blood/article-pdf/98/4/1003/1676353/h8160101003.pdf by guest on 05 June 2024

CD34 (Pharmingen). Cells were washed 3 times with FACS buffer and resuspended in 500 μL FACS buffer before analysis on a FACSort (Becton Dickinson, Mountain View, CA) flow cytometer equipped with CellQuest software (Becton Dickinson). The viable cells that remained unstained represented hepatocytes, whereas the $CD11b^+$ population included Kupffer cells and contaminating PB phagocytes. For BM samples, the percent staining was multiplied by the total cellularity (obtained from one femur) to determine the absolute number of each cell type.

Chromosome analysis

For $Fancc^{+/+}Sod1^{+/+}$, $Fancc^{+/-}Sod1^{+/-}$, and $Fancc^{-/-}Sod1^{-/-}$ BM samples, an aliquot of RPMI + 5% FCS containing 1.5×10^6 resuspended BM cells was added to a tube containing 1 mL trypsin-EDTA (Irvine Scientific, Santa Ana, CA) and 0.75 M KCl. The tubes were incubated at 37°C for 25 minutes, spun for 10 minutes at 1000 rpm and the pellet carefully resuspended in Carnoy fixative (3 parts methanol to 1 part glacial acetic acid). The fixative was changed 2 more times and the slides made by air-drying. Approximately 10 metaphases per sample were examined for evidence of chromosomal breaks, gaps, or detectable rearrangements.

Methylcellulose colony-forming assays and lineage depletion of total BM cells

Whole BM cells were plated in 1.1 mL 1% methylcellulose media supplemented with 10% FCS, 2 mM L-glutamine, 10^{-4} M 2-mercaptoethanol and the following recombinant growth factors: for myeloid assays, methylcellulose was supplemented with 1% BSA, 10 μg/mL bovine pancreatic insulin, 200 μg/mL human transferrin, 3 U/mL recombinant human erythropoietin, 10 ng/mL recombinant mouse interleukin (IL)-3, 10 ng/mL recombinant human IL-6, and 50 ng/mL recombinant mouse stem cell factor (SCF). For pre-B assays 10 ng/mL recombinant human IL-7 was used (Stem Cell Technologies, Vancouver, BC). Cells were dispensed using a blunt-ended needle and cultured at a density of 1.7×10^5 and 5.5×10^4 cells/35-mm dish for pre-B and myeloid colonies, respectively (each sample done in duplicate). Dishes were incubated for 6 (for pre-B) or 12 (for myeloid) days at 37°C, 5% CO_2 in air, ≥ 95% humidity. Colonies (> 20 cells) were counted on a gridded stage using an inverted light microscope. Lineage-depleted (Lin^-) samples were collected by resuspending the cells at 5.0×10^7 nucleated cells/mL in PBS with 2% FBS, plus 5% rat serum for 15 minutes at 4°C. Samples were first incubated with an antibody cocktail (CD5, CD11b, CD45R, GR1, 7-4, and TER-119) and subsequently with an antibiotin tetrameric antibody (both antibody cocktails from Stem Cell Technologies) complex (each step for 15 minutes at 4°C); then a magnetic colloid was added for cell separation as recommended (Stem Cell Technologies). To isolate Lin^- populations, the suspension was applied to a primed 0.3-inch magnetic column and washed 3 times with PBS containing 2% FBS. The cells in the flow-through were enumerated and trypan blue exclusion used to determine viability (>95%).

Statistical methods

The Student *t* test (Microsoft Excel) was used when analyzing the results. A *P* value less than .05 was considered significant.

Results

Fancc$^{-/-}$*Sod1*$^{-/-}$ mice develop zonal microvesicular hepatic steatosis

No developmental defects or gross skeletal abnormalities were seen in $Fancc^{-/-}Sod1^{-/-}$ mice. Body weights of $Fancc^{-/-}$, $Sod1^{-/-}$, $Fancc^{+/-}Sod1^{+/-}$, $Fancc^{+/+}Sod1^{+/+}$, and $Fancc^{-/-}Sod1^{-/-}$ mice, both male and female, were not statistically different from one another (data not shown). Liver and spleen weights were not increased in any of the mutants as compared to $Fancc^{+/+}Sod1^{+/+}$ controls. However, necropsy and histologic analysis of $Fancc^{-/-}Sod1^{-/-}$ mice revealed abnormalities of the liver and BM.

On inspection, livers of $Fancc^{-/-}Sod1^{-/-}$ mice (n = 6) were pale and exhibited a yellow reticular surface pattern (data not shown). Liver sections were examined by light and electron microscopy, with a typical sample shown in Figure 1. Liver sections from $Fancc^{-/-}$ (Figure 1A,E), $Sod1^{-/-}$ (Figure 1B,F), $Fancc^{+/-}Sod1^{+/-}$ (Figure 1C,G), and $Fancc^{-/-}Sod1^{-/-}$ (Figure 1D,H) mice were stained with Mason trichrome (Figure 1A-D). Whereas periportal (zones 1 and 2) hepatocytes were unremarkable, zone 3 cells were distended by numerous periodic acid-Schiff–negative (data not shown) cytoplasmic vacuoles that did not displace the nuclei. No inflammatory cell infiltrates were present in the liver, and trichrome stain did not reveal evidence of hepatic fibrosis or increased collagen deposition. Staining with oil red-O (Figure 1E-H) demonstrated microvesicular steatosis (Figure 1H) in zone 3 hepatocytes of $Fancc^{-/-}Sod1^{-/-}$ mice. $Fancc^{-/-}$ mice (Figure 1E) revealed no increase in lipid staining over controls, whereas $Sod1^{-/-}$ mice (Figure 1F) revealed modest amounts of oil red O-positive droplets distributed in a nonzonal pattern. Transmission electron microscopy, performed on $Fancc^{+/-}Sod1^{+/-}$ (Figure

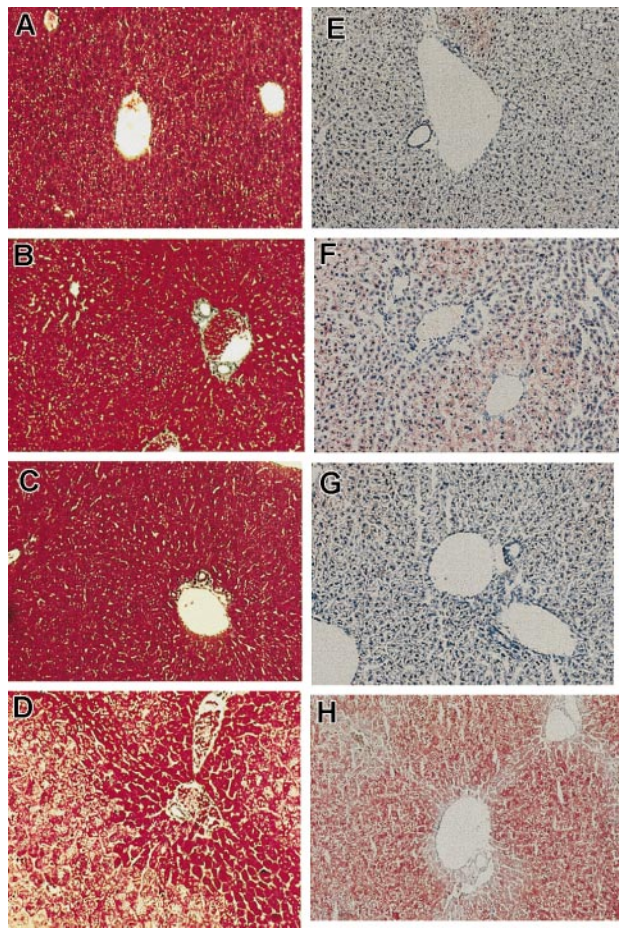

Figure 1. Histologic examination reveals zonal hepatic microvesicular steatosis in *Fancc*$^{-/-}$*Sod1*$^{-/-}$ mice. Histology of $Fancc^{-/-}Sod1^{-/-}$ and control livers (magnification × 400). Sections of $Fancc^{-/-}$(A,E), $Sod1^{-/-}$(B,F), $Fancc^{+/-}Sod1^{+/-}$ (C,G), and $Fancc^{-/-}Sod1^{-/-}$ (D,H) livers were stained with Masson trichrome (A-D) and oil red-O (E-H). Whereas $Fancc^{-/-}$, $Sod1^{-/-}$, and $Fancc^{+/-}Sod1^{+/-}$cells show normal morphology, $Fancc^{-/-}Sod1^{-/-}$ hepatocytes demonstrate a zone 3 abnormality characterized by abundant cytoplasmic vacuolation. Staining with oil red-O demonstrates prominent microvesicular zone 3 lipid accumulation without nuclear displacement in $Fancc^{-/-}Sod1^{-/-}$ mice. Small amounts of lipid droplets are present in $Sod1^{-/-}$ mice.

Downloaded from http://ashpublications.net/blood/article-pdf/98/4/1003/1676353/h8160101003.pdf by guest on 05 June 2024

2A,C) and *Fancc*$^{-/-}$*Sod1*$^{-/-}$ (Figure 2B,D) liver samples, revealed no morphologic abnormalities of Kupffer cells or endothelial sinusoidal cells, and aside from the obvious lipid-filled vacuoles, the structure of hepatocyte smooth endoplasmic reticulum and mitochondria was unremarkable (Figure 2C-D).

To search for evidence of hepatocyte injury, serum ALT and TUNEL were used. ALT levels were as follows: *Sod1*$^{-/-}$, 55.3 ± 8.67; *Fancc*$^{-/-}$, 45.5 ± 2.87; *Fancc*$^{+/+}$*Sod1*$^{+/+}$, 41.3 ± 7.98; *Fancc*$^{+/-}$ *Sod1*$^{+/-}$, 22.7 ± 4.2; and *Fancc*$^{-/-}$*Sod1*$^{-/-}$, 126.8 ± 52.0. Although the serum ALT level from *Fancc*$^{-/-}$*Sod1*$^{-/-}$ mice was increased (~3-fold) over littermate controls, suggesting that low levels of hepatocyte damage may have been present, these data are not statistically significant ($P = .12$). TUNEL assay of liver sections revealed no difference with respect to the rare apoptotic cells seen when *Fancc*$^{-/-}$ *Sod1*$^{-/-}$ and littermate mice were compared (data not shown).

Primary *Fancc*$^{-/-}$*Sod1*$^{-/-}$ liver cell cultures generate increased levels of superoxide

To search for evidence of oxidant stress in *Fancc*$^{-/-}$*Sod1*$^{-/-}$ livers, we assayed spontaneous superoxide production from primary liver cell cultures. Luminol, which undergoes chemiluminescence when oxidized by superoxide, enabled quantitation of the relative amounts of this species. The average intensity of the samples was recorded as RLUs, with the RLU values being proportional to the level of superoxide in the samples. Figure 3 shows the average RLU values for 5 mice per group, each mouse sample assayed in triplicate, taken immediately after luminol addition. In all samples, the luminol signal was ablated when SOD protein was added to the culture medium (data not shown). *Fancc*$^{+/+}$*Sod1*$^{+/+}$, *Fancc*$^{-/-}$, and *Fancc*$^{+/-}$*Sod1*$^{+/-}$ controls all had statistically similar RLU values of 0.33, 0.38, and 0.44, respectively. *Sod1*$^{-/-}$ samples showed a marginally elevated RLU value of 0.52 that was statistically different from *Fancc*$^{+/+}$*Sod1*$^{+/+}$ mice ($P = .01$).

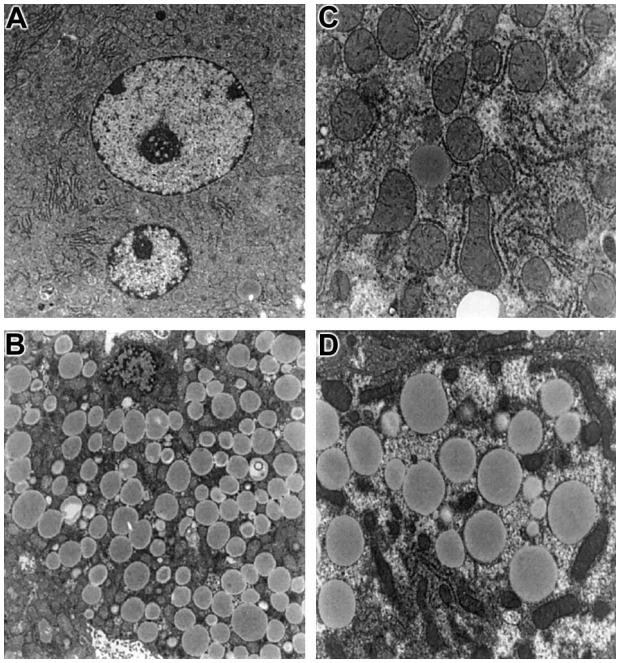

Figure 2. Electron microscopy of hepatocytes from *Fancc*$^{-/-}$*Sod1*$^{-/-}$ mice reveals no increase in organelle damage. Hepatocytes from *Fancc*$^{+/-}$*Sod1*$^{+/-}$ (A,C) and *Fancc*$^{-/-}$*Sod1*$^{-/-}$ (B,D) mice stained with osmium tetroxide. (A) A normal multinucleated centrilobular hepatocyte (× 5400) and (C) a higher magnification showing normal organelles (× 11 750). (B) Microvesicular steatosis in a centrilobular *Fancc*$^{-/-}$*Sod1*$^{-/-}$ hepatocyte (× 5400) and (D) (× 11 750).

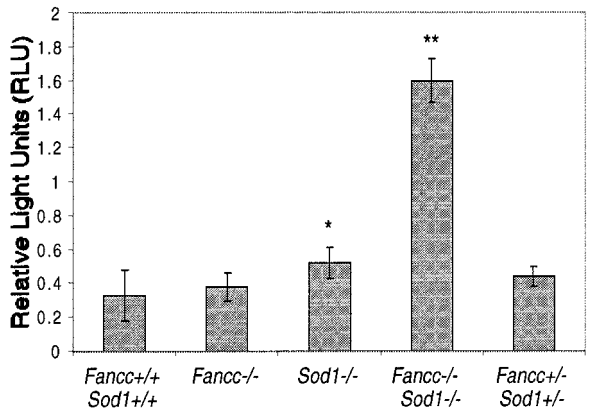

Figure 3. Primary hepatocytes have an increase in superoxide levels detected by luminol-dependent chemiluminescence. The level of superoxide is reflected by the RLU value. Each bar represents the mean ± SEM for 5 mice per group, with each sample in triplicate. *, $P < .05$; **, $P < .001$ by the Student *t* test.

In contrast, there was a 4.8-fold increase in the RLU value obtained from *Fancc*$^{-/-}$*Sod1*$^{-/-}$ cells (1.62) compared with *Fancc*$^{+/+}$*Sod1*$^{+/+}$ controls ($P = .0008$). Although hepatocytes were likely the source of the increased levels of superoxide in *Fancc*$^{-/-}$*Sod1*$^{-/-}$ cells, we are unable to define the potential contribution of Kupffer cell-derived superoxide. FACS analysis demonstrated that the percentage of CD11b^{+} cells was similar in all samples (data not shown).

Increased expression of manganese SOD and heme-oxygenase-1 in *Fancc*$^{-/-}$*Sod1*$^{-/-}$ livers

Heme-oxygenase-1 is induced by various cellular stressors, including ROS.[31,32] Similarly, manganese SOD (MnSOD) can also be induced by ROS, including superoxide.[33,34] Thus, an increased level of MnSOD or heme-oxygenase-1 (HO-1) in total liver cell lysates, as assessed by immunoblotting with anti-MnSOD and HO-1 antibodies, would be predicted to accompany the putative prooxidant state in *Fancc*$^{-/-}$*Sod1*$^{-/-}$ hepatocytes. Figure 4 represents protein levels of HO-1 and MnSOD in lysates from *Fancc*$^{+/+}$*Sod1*$^{+/+}$, *Fancc*$^{+/-}$*Sod1*$^{+/-}$, and *Fancc*$^{-/-}$*Sod1*$^{-/-}$ mice. Densitometric analysis of a number of immunoblotting experiments was carried out, with the ratio of protein band intensities for MnSOD or HO-1 normalized according to band intensities following stripping and reimmunoblotting of the same filters with an anti–β-tubulin antibody. The results demonstrate increased levels of MnSOD and

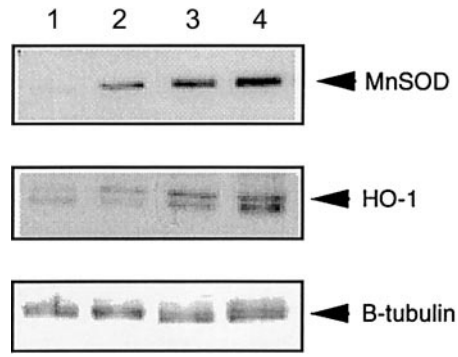

Figure 4. Liver-specific expression of MnSOD and HO-1 is increased in *Fancc*$^{-/-}$*Sod1*$^{-/-}$ mice. Autoradiographs showing total liver lysates immunoblotted with antibodies against MnSOD and HO-1, and normalized for loading with anti–β-tubulin antibody. Lane 1 control (Stressgen Biotech, Victoria, British Columbia, Canada), lane 2 *Fancc*$^{+/+}$*Sod1*$^{+/+}$, lane 3 *Fancc*$^{+/-}$*Sod1*$^{+/-}$, and lane 4 *Fancc*$^{-/-}$*Sod1*$^{-/-}$ liver lysates.

Downloaded from http://ashpublications.net/blood/article-pdf/98/4/1003/1676353/h8160101003.pdf by guest on 05 June 2024

Table 1. Peripheral blood values from mice aged 8 to 10 weeks

		CBC Values‡				
Genotype	n	RBCs (10^{12}/L)	WBCs (10^9/L)	Hgb (g/L)	PLTs (10^9/L)	MCV (fL)
Fancc$^{+/+}$*Sod1*$^{+/+}$	15	10.02 ± 0.27	3.69 ± 1.09	163.4 ± 4.47	605.3 ± 47.2	52.8 ± 0.69
Fancc$^{+/-}$*Sod1*$^{+/-}$	18	9.66 ± 0.27	6.59 ± 0.86	161.9 ± 4.50	708 ± 49.3	52.3 ± 0.62
Fancc$^{-/-}$	9	9.68 ± 0.20	1.55 ± 0.23	158.6 ± 4.05	435 ± 26.9*	53.5 ± 0.42
Sod1$^{-/-}$	10	8.72 ± 0.42*	1.94 ± 0.56	147 ± 3.96*	745.5 ± 49.1	54.1 ± 1.0
Fancc$^{-/-}$*Sod1*$^{-/-}$	9	7.9 ± 0.36†	0.96 ± 0.20*	136 ± 4.52†	719 ± 93.7	58.5 ± 0.68†

Values represent average ± SEM for the indicated number of animals per group.
RBC indicates red blood cells; WBC, white blood cells; CBC, complete blood count; Hgb, hemoglobin; PLTs, platelets; MCV, mean cell volume.
*$P < .05$.
†$P < .0005$.
‡CBCs were quantified using a Sysmex 9500 automated blood analyser.

HO-1 of about 4-fold and 10-fold, respectively, in *Fancc*$^{-/-}$ *Sod1*$^{-/-}$ livers, as compared with *Fancc*$^{+/+}$*Sod1*$^{+/+}$ littermates, consistent with in vivo oxidative stress.

PB and BM abnormalities of *Fancc*$^{-/-}$*Sod1*$^{-/-}$ mice

To search for evidence of BM dysfunction, we evaluated PB cells from *Fancc*$^{+/+}$*Sod1*$^{+/+}$, *Fancc*$^{+/-}$*Sod1*$^{+/-}$, *Fancc*$^{-/-}$, *Sod1*$^{-/-}$, and *Fancc*$^{-/-}$*Sod1*$^{-/-}$ mice (Table 1). Significant decreases were observed in the RBC ($P = .005$) and WBC ($P = .03$) compartments of *Fancc*$^{-/-}$*Sod1*$^{-/-}$ mice, as compared with *Fancc*$^{+/+}$ *Sod1*$^{+/+}$ littermates. WBC values from *Fancc*$^{-/-}$, *Sod1*$^{-/-}$, and *Fancc*$^{-/-}$*Sod1*$^{-/-}$ mice, however, were not significantly different from one another ($P = .18$ and $P = .12$, respectively). *Fancc*$^{-/-}$ *Sod1*$^{-/-}$ differentials (n = 4) revealed that the WBC decrease was due to a reduction in both neutrophils and lymphocytes. There was no indication of a granulocyte maturation arrest in any of the samples. PB smears revealed that lymphocytes from *Fancc*$^{-/-}$ *Sod1*$^{-/-}$ blood were often larger with more immature nuclear chromatin then either *Fancc*$^{+/+}$*Sod1*$^{+/+}$ or *Fancc*$^{+/-}$*Sod1*$^{+/-}$ controls. Erythrocyte MCV was significantly increased ($P < .00001$), and there were higher numbers of polychromatic RBCs in *Fancc*$^{-/-}$ *Sod1*$^{-/-}$ mice compared with controls (data not shown). *Fancc*$^{-/-}$ mice demonstrated a trend toward reduced WBC counts; however, this decrease was not significant ($P = .07$). Platelet counts were normal in *Fancc*$^{-/-}$*Sod1*$^{-/-}$ mice, consistent with the normal megakaryocyte numbers observed in the marrow. Interestingly, 8-week-old, but not older (platelet count 587 ± 12.9) *Fancc*$^{-/-}$ mice showed a significant ($P = .007$) decrease in platelet numbers. Furthermore, there were reductions in both RBC ($P = .03$) and hemoglobin ($P = .04$) values in *Sod1*$^{-/-}$ mice, as compared with *Fancc*$^{+/+}$*Sod1*$^{+/+}$ controls. Peripheral counts were obtained from mice up to the age of 3 months. With age, WBC values from *Fancc*$^{-/-}$ mice (10.5 ± 1.5) increase to *Fancc*$^{+/+}$*Sod1*$^{+/+}$ levels (10.21 ± 0.86), ceasing to be statistically similar to WBC values from *Fancc*$^{-/-}$*Sod1*$^{-/-}$ mice (5.9 ± 0.86). Thus, in contrast to *Fancc*$^{-/-}$*Sod1*$^{-/-}$ mice, the reductions of WBCs and RBCs seen in 8- to 10-week-old *Fancc*$^{-/-}$ mice normalize over time.

The BMs of *Fancc*$^{+/-}$*Sod1*$^{+-}$, *Fancc*$^{-/-}$, *Sod1*$^{-/-}$, and *Fancc*$^{-/-}$ *Sod1*$^{-/-}$ femurs were next assessed (representative examples are shown in Figure 5). Decreased cellularity was present in *Fancc*$^{-/-}$ *Sod1*$^{-/-}$, suggested by increased fat cell numbers, particularly in the long bone metaphyses. In 5 of 5 *Fancc*$^{-/-}$*Sod1*$^{-/-}$ femurs analyzed, a large increase in the amount of BM fat was present, whereas in only 1 of 4 *Fancc*$^{+/+}$*Sod1*$^{+/+}$ and 1 of 4 *Fancc*$^{+/-}$ *Sod1*$^{+/-}$ controls there was an increase in fat, and when present this was less pronounced than that of *Fancc*$^{-/-}$*Sod1*$^{-/-}$ mice. Total BM cell numbers per femur were obtained from *Fancc*$^{+/+}$*Sod1*$^{+/+}$, *Fancc*$^{+/-}$*Sod1*$^{+/-}$, *Fancc*$^{-/-}$, *Sod1*$^{-/-}$, and *Fancc*$^{-/-}$*Sod1*$^{-/-}$ mice (Table 2; n is as shown). Cellularity was decreased in *Fancc*$^{-/-}$ *Sod1*$^{-/-}$ mice ($2.33 \times 10^7 \pm 0.19$) compared with *Fancc*$^{+/+}$ *Sod1*$^{+/+}$ controls ($3.98 \times 10^7 \pm 0.62$) by 58%; however, this was not significant ($P = .06$). There was also no statistical difference in total BM cellularity between *Fancc*$^{+/-}$*Sod1*$^{+/-}$, *Fancc*$^{-/-}$, and *Sod1*$^{-/-}$ controls. To determine whether any specific BM cell type might be differentially affected, flow cytometry was carried out on total BM samples with the following monoclonal antibodies: PGP1, B220, Ly6G, 7-4, CD11b, CD14, and Ter-119. As shown in Table 2, the average number of *Fancc*$^{-/-}$*Sod1*$^{-/-}$ cells of each type was decreased by at least 40%, as compared with *Fancc*$^{+/+}$ *Sod1*$^{+/+}$ controls. To investigate whether these reductions were mirrored by reduced numbers of committed (Lin$^+$) progenitors, Lin$^+$Sca1$^+$, Lin$^+$ckit$^+$ and Lin$^+$CD34$^+$ values were obtained from *Fancc*$^{+/-}$*Sod1*$^{+/-}$ and *Fancc*$^{-/-}$*Sod1*$^{-/-}$ mice (n = 3). The average absolute number of these progenitor populations for *Fancc*$^{+/-}$ *Sod1*$^{+/-}$ mice was 1.8×10^6, 3.6×10^6, and 1.7×10^6, and for *Fancc*$^{-/-}$*Sod1*$^{-/-}$mice, 0.9×10^6, 1.26×10^6, and 0.8×10^6, respectively, demonstrating that committed progenitor populations were decreased in *Fancc*$^{-/-}$*Sod1*$^{-/-}$ BMs. There was no evidence of increased extramedullary hematopoiesis, because spleens obtained from 2 sets of animals revealed no change in cellularity:

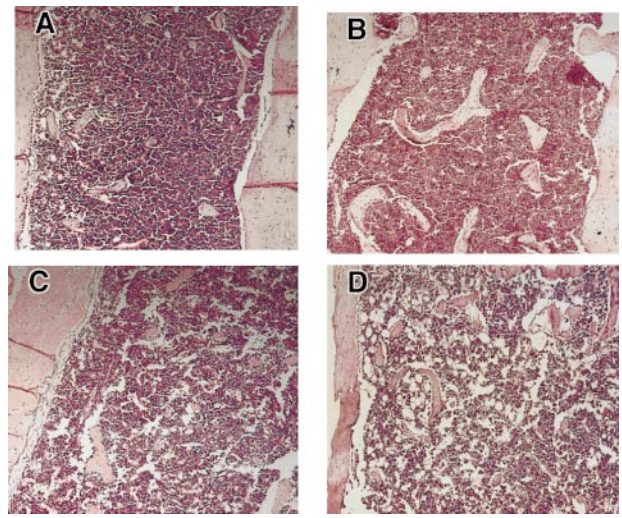

Figure 5. Hypocellularity and increased fat accumulation in *Fancc*$^{-/-}$*Sod1*$^{-/-}$ BM. Metaphyseal sections of leg bones from *Fancc*$^{+/+}$*Sod1*$^{+/+}$ (A), *Fancc*$^{-/-}$ (B), *Sod1*$^{-/-}$ (C), and *Fancc*$^{-/-}$*Sod1*$^{-/-}$ (D) mice (magnification × 400). Marrow fat content (clear areas) is increased in *Fancc*$^{-/-}$*Sod1*$^{-/-}$ mice compared with *Fancc*$^{+/+}$ *Sod1*$^{+/+}$ or to *Fancc*$^{-/-}$. Controls revealed only rare fat cells,whereas *Sod1*$^{-/-}$ mice did show some increase in fat spaces.

Downloaded from http://ashpublications.net/blood/article-pdf/98/4/1003/1676353/h8160101003.pdf by guest on 05 June 2024

Table 2. Total bone marrow cellularity and absolute number of cell types from mice aged 8 to 10 weeks

Genotype	n	Average cellularity/femur (10^7)	mAb (Absolute cell no. 10^7)						
			PGP1	B220	Ly6G	CD11b	CD14	PMN	Ter-119
Fancc$^{+/+}$*Sod1*$^{+/+}$	6	3.98 ± 0.62	2.89	0.86	1.28	1.33	0.05	1.21	1.36
Fancc$^{+/-}$*Sod1*$^{+/-}$	7	4.08 ± 0.57	3.14	1.21	1.48	1.42	0.14	1.46	1.30
Fancc$^{-/-}$	6	3.41 ± 0.33	2.21	0.77	0.87	0.77	0.04	0.73	1.2
Sod1$^{-/-}$	5	3.53 ± 0.57	2.7	0.88	1.23	1.2	0.06	1.1	1.05
Fancc$^{-/-}$*Sod1*$^{-/-}$	6	2.33 ± 0.19	1.68	0.56	0.79	0.73	0.01	0.85	0.72

Average BM cellularity/femur is represented as the average ± SEM. *Fancc*$^{-/-}$*Sod1*$^{-/-}$ cellularity was decreased by approximately 52% compared with *Fancc*$^{+/-}$*Sod1*$^{+/-}$ ($P = .08$). Absolute numbers represent the average % staining × average cellularity and was consistantly reduced by a minimum of 40% compared with *Fancc*$^{+/-}$*Sod1*$^{+/-}$ controls. Cellularity was decreased in *Sod1*$^{-/-}$ and *Fancc*$^{-/-}$ mice as well.

Fancc$^{-/-}$*Sod1*$^{-/-}$ ($9.65 \times 10^7 \pm 0.45$) and *Fancc*$^{+/-}$*Sod1*$^{+/-}$ ($13 \times 10^7 \pm 3.85$).

Fancc$^{-/-}$*Sod1*$^{-/-}$ total BM cells fail to show increased apoptosis or chromosomal aberrations

Because BM hypocellularity in *Fancc*$^{-/-}$*Sod1*$^{-/-}$ mice may have been due to an increased level of apoptosis, total BM samples were analyzed by flow cytometry and propidium iodide/annexinV (PI/A) staining. However, this revealed no gross increase in apoptotic cells in *Fancc*$^{-/-}$*Sod1*$^{-/-}$ mice, as compared with *Fancc*$^{+/-}$*Sod1*$^{+/-}$ controls (Table 3). Although suggesting that increased apoptosis might not be the explanation for the BM hypocellularity, the possibility of increased apoptosis within a progenitor subset was not excluded by this procedure. Because gross cytogenetic abnormalities would impair hematopoietic cell development, we evaluated metaphase chromosome spreads from *Fancc*$^{+/+}$*Sod1*$^{+/+}$, *Fancc*$^{+/-}$*Sod1*$^{+/-}$, and *Fancc*$^{-/-}$*Sod1*$^{-/-}$ BM cells. However, there was no evidence of increased chromosomal aberrations (breaks, gaps, or detectable rearrangements) in *Fancc*$^{-/-}$*Sod1*$^{-/-}$ mice (n = 2) as compared with control mice (n = 3) on examination of 10 metaphase cells per mouse (data not shown).

In vitro hematopoietic colony growth is severely impaired in *Fancc*$^{-/-}$*Sod1*$^{-/-}$ mice

Because BM hypocellularity might result from inadequate growth of hematopoietic progenitors in *Fancc*$^{-/-}$*Sod1*$^{-/-}$ mice, we examined the in vitro clonogenic potential of committed myeloid (granulocyte-macrophage colony-forming units [CFU-GMs]) and lymphoid (pre-B colony-forming units [CFU-pre-Bs]) progenitors from *Sod1*$^{-/-}$, *Fancc*$^{-/-}$, *Fancc*$^{+/+}$*Sod1*$^{+/+}$, *Fancc*$^{+/-}$*Sod1*$^{+/-}$, and *Fancc*$^{-/-}$*Sod1*$^{-/-}$ mice. Figure 6A represents the average number of progenitors/femur ± SEM from myeloid (dark bars) and pre-B (hatched bars) methylcellulose assays for n = 6 to 8 animals per genotype, with each experiment done in duplicate (for *Sod1*$^{-/-}$ pre-B cultures, n = 4). These data clearly show that the numbers of colonies from myeloid and pre-B progenitors/femur from *Fancc*$^{-/-}$ *Sod1*$^{-/-}$ mice ($P = .0002$ for both) was severely depressed, as compared with *Fancc*$^{+/+}$*Sod1*$^{+/+}$ controls. The data indicate that the number of myeloid and pre-B progenitors/femur from *Fancc*$^{-/-}$ *Sod1*$^{-/-}$ mice was approximately 75-fold lower than that from *Fancc*$^{+/+}$*Sod1*$^{+/+}$ controls. Interestingly, the number of colonies obtained from *Sod1*$^{-/-}$ and *Fancc*$^{-/-}$ BM samples was also significantly reduced ($P = .04$ and $P = .01$, respectively) for both

Table 3. PI/Annexin FACS Analysis from total bone marrow samples

Genotype	n	% Staining	
		Annexin$^+$ PI$^-$	Annexin$^+$ PI$^+$
Fancc$^{+/-}$ *Sod1*$^{+/-}$	5	25.49 ± 4.59	15.52 ± 3.08
Fancc$^{-/-}$ *Sod1*$^{-/-}$	5	28.38 ± 3.83	16.44 ± 6.12

FACS Staining was used to quantitate the number of apoptotic cells from total BM samples of 8-9 week old mice. Annexin$^+$/PI$^-$ values represent cells initiating the apoptotic process and Annexin$^+$/PI$^+$ values represent cells that have already undergone apoptosis and death.

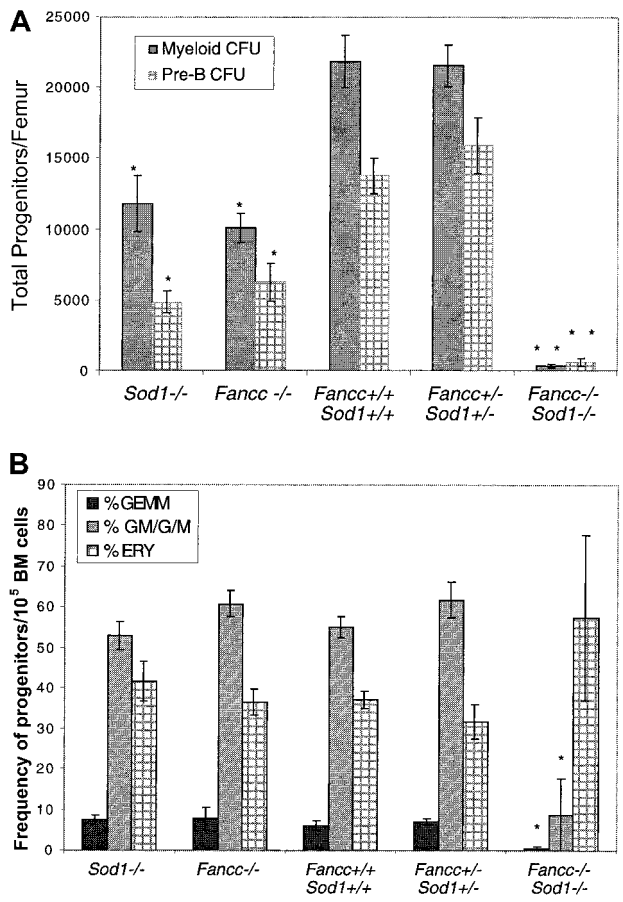

Figure 6. Colony-forming assays. (A) Colony-forming assays reveal decreased numbers of progenitors in *Fancc*$^{-/-}$*Sod1*$^{-/-}$ BM samples. Myeloid (dark bars) and pre-B (hatched bars) CFUs were determined for *Sod1*$^{-/-}$, *Fancc*$^{-/-}$, *Fancc*$^{+/+}$ *Sod1*$^{+/+}$, *Fancc*$^{+/-}$*Sod1*$^{+/-}$, and *Fancc*$^{-/-}$*Sod1*$^{-/-}$ mice. The decrease in the number of progenitors/femur is highly significant ($P = .0002$) when *Fancc*$^{-/-}$*Sod1*$^{-/-}$ mice are compared to *Fancc*$^{+/+}$*Sod1*$^{+/+}$ controls. Values represent the average number of progenitors/femur of 6 mice per group ± SEM. * = $P < .05$, ** = $P < .001$. (B) *Fancc*$^{-/-}$*Sod1*$^{-/-}$ progenitors fail to generate normal ratios of CFU-GEMM, CFU-GM/G/M, and BFU-E. Myeloid colonies from panel A were assessed morphologically to determine the cell types contributing to the colonies. CFU-GEMM (dark bars), CFU-GM/G/M (light gray bars), and BFU-E (hatched bars) colonies were scored by eye and the values represent average percent of cell type ± SEM (n = 6-8 mice/group). Ratios of CFU-GM/G/M, and CFU-GEMM from *Fancc*$^{-/-}$*Sod1*$^{-/-}$ samples were significantly different from *Fancc*$^{+/+}$*Sod1*$^{+/+}$ controls ($P = .002$ and $P = .003$, respectively).

Downloaded from http://ashpublications.net/blood/article-pdf/98/4/1003/1676353/h8160101003.pdf by guest on 05 June 2024

the myeloid and pre-B assays when compared with $Fancc^{+/+}$ $Sod1^{+/+}$ and $Fancc^{+/-}Sod1^{+/-}$ controls.

In vitro colony-forming assays provide additional information about the quality of committed progenitors because both the size of the colonies as well as the frequency of different cell types arising from a myeloid progenitor can be evaluated. For example, most colonies scored from $Fancc^{-/-}Sod1^{-/-}$ mice just met the criteria for colony size (> 20 cells/colony), as compared with colonies from $Fancc^{+/+}Sod1^{+/+}$ controls, which were highly cellular. Furthermore, the colonies described in Figure 6A were scored by cell morphology into granulocyte, erythrocyte, macrophage, megakaryocyte colony-forming unit (CFU-GEMM), CFU-GM/G/M, and erythroid burst forming unit (BFU-E) groups. Figure 6B represents the frequency of progenitors/10^5 BM cells. We found that colonies enumerated from $Fancc^{-/-}Sod1^{-/-}$ samples were mostly erythroid in origin, 57.4% ± 20.44% ($P = 0.12$) with very few CFU-GM/G/M, 8.78% ± 8.0%, and CFU-GEMM, 0.46% ± 0.21%, colonies being present ($P = .002$ and $P = .003$, respectively). $Sod1^{-/-}$, $Fancc^{-/-}$, $Fancc^{+/+}Sod1^{+/+}$, $Fancc^{+/-}Sod1^{+/-}$ progenitors, on the other hand, all gave rise to the different cell types at similar frequencies. It was also important to determine whether plating increased numbers of cells would augment colony formation by $Fancc^{-/-}Sod1^{-/-}$ BM samples. However, plating at concentrations of 2, 5, or 10 times the original cell number did not augment growth of $Fancc^{-/-}Sod1^{-/-}$ colony-forming cells (data not shown), suggestive of toxicity, or an inadequate response to exogenous growth factors. Although cells from individuals with FA can be sensitive to ambient oxygen, subjecting the $Fancc^{-/-}Sod1^{-/-}$ BM cultures to 5% O_2 also did not augment colony growth (data not shown). The latter 2 experiments represent 3 mice for each of $Fancc^{-/-}Sod1^{-/-}$ and $Fancc^{+/-}Sod1^{+/-}$, with each experiment performed in duplicate.

Primitive progenitor numbers are normal in $Fancc^{-/-}Sod1^{-/-}$ mice

Although BM hypocellularity could result from reduced levels of early progenitors, $Fancc^{-/-}Sod1^{-/-}$ BM samples did not exhibit a significant reduction in the Lin^- compartment. Thus, the absolute number of Lin^- cells, as determined by flow cytometry of nonfractionated total BM samples, was similar for $Fancc^{+/-}$ $Sod1^{+/-}$ ($1.7 \times 10^5 \pm 0.3$/femur) and $Fancc^{-/-}Sod1^{-/-}$ mice ($1.3 \times 10^5 \pm 0.7$/femur); n = 3 in each case. Furthermore, the absolute number of Lin^- cells (obtained after Lin^+ cell depletion-column experiments) from $Fancc^{+/-}Sod1^{+/-}$ controls ($7.6 \times 10^5 \pm 1.52$) was similar to that of $Fancc^{-/-}Sod1^{-/-}$ mice ($5.2 \times 10^5 \pm 1.05$); n = 6 (values represent cell numbers obtained from both femurs and tibiae per mouse). Flow cytometry of Lin^- cells, obtained following Lin^+ depletion, using monoclonal antibodies against CD34, Sca1 and c-kit revealed no significant differences. The values below represent experiments using 5 animals per group and are the average absolute number ± SEM. Thus, the absolute number of $Lin^-Sca1^+c\text{-}kit^-$ and $Lin^-Sca1^+c\text{-}kit^+$ cells from $Fancc^{-/-}Sod1^{-/-}$ mice was $1.3 \times 10^4 \pm 0.3$ and $5.1 \times 10^4 \pm 2.0$, whereas for $Fancc^{+/-}Sod1^{+/-}$ controls, values were $2.0 \times 10^4 \pm 0.9$ and $3.4 \times 10^4 \pm 0.9$, respectively. The similarity is also observed in the $Lin^-CD34^+Sca1^-$ compartment, where both $Fancc^{-/-}Sod1^{-/-}$ mice and $Fancc^{+/-}Sod1^{+/-}$ controls had $13 \times 10^5 \pm 0.7$ cells. We conclude that the absolute number of cells within the Lin^- compartment of $Fancc^{-/-}Sod1^{-/-}$ BM is similar to controls and that progenitor subpopulations within the Lin^- compartment of these mice are also similar to controls.

Discussion

Herein we show that mice having combined deficiencies of Fancc and the primary cytosolic superoxide-detoxifying enzyme, Sod1, exhibit 2 novel phenotypes: fatty liver and an impairment of hematopoietic cell development.

$Fancc^{-/-}Sod1^{-/-}$ liver pathology was characterized primarily by zone 3 microvesicular steatosis, possibly a manifestation of in vivo superoxide toxicity as evidenced by increased superoxide production. In keeping with superoxide-mediated pathology, we found increases in the oxidative stress-inducible enzymes, MnSOD and HO-1, within $Fancc^{-/-}Sod1^{-/-}$ livers. Although microvesicular fatty liver is often encountered as a result of mitochondrial dysfunction, it can also result from impaired egress of lipids from hepatocytes as seen following specific hepatotoxin exposures.[35] ROS, such as superoxide, either alone, or in combination with nitric oxide (NO) to yield peroxynitrite ($ONOO^-$),[36] are able to react with a variety of cellular macromolecules, including membrane lipids.[37] Lipid peroxidation and accumulated hydroxy fatty acids[38] within membranes of the endoplasmic reticulum, for example, can interfere with transport of lipids or components of very-low-density lipoprotein particles that are responsible for removing lipids from hepatocytes.[35] Interestingly, and possibly in keeping with superoxide-mediated organelle, and possibly plasma membrane damage, the livers of mice lacking MnSOD (Sod2) also demonstrated microvesicular steatosis[39] and increased levels of serum ALT. It should also be noted that ROS can function as second messengers, modulating the activities of intracellular signaling molecules and transcription factors.[40,41] Thus, liver pathology in $Fancc^{-/-}Sod1^{-/-}$ mice might stem from abnormal gene expression patterns secondary to elevated superoxide levels or reduced dismutation of this species into hydrogen peroxide.

Increased superoxide production by $Fancc^{-/-}Sod1^{-/-}$ liver cell cultures was interesting given the reports of elevated ROS generation by FA cells,[21,22] and the reported protective effects of SOD, where extrinsic SOD reduced the high rates of chromosomal breakage in FA cells, and also diminished MMC cytotoxicity.[16,42,43] Interestingly, reduced SOD1 levels have been reported in FA erythrocytes.[44-46] Unlike the $Fancc^{-/-}Sod1^{-/-}$ cross, hepatic steatosis has not been reported in human FA. Assuming that a similar pathogenetic mechanism were involved in FA, this discordance might be explained by the species-specific differences in CYP P-450 genes or xenobiotic exposure.

Because lipid accumulation in hepatocytes can be accompanied by necrosis[47] and inflammatory infiltrates, we searched for evidence of hepatocyte damage and cellular infiltrates. Only the modest elevations of serum ALT were suggestive of hepatocyte damage, and this occurred in the absence of overt necrosis or pathologic collagen deposition. Activation of Kupffer cells, which also leads to ROS, NO, as well as proinflammatory cytokine production, can injure hepatocytes, and is often accompanied by neutrophil infiltration.[37] The lack of infiltrates, the normal percentages of $CD11b^+$ cells in $Fancc^{-/-}Sod1^{-/-}$ liver samples, and the zonal liver pathology, however, would suggest a defect intrinsic to the hepatocytes of $Fancc^{-/-}Sod1^{-/-}$ mice.

The second phenotype of $Fancc^{-/-}Sod1^{-/-}$ mice was that of marrow hypoplasia, accompanied by a striking impairment of in vitro hematopoietic colony formation. Given the normal levels of primitive precursors, this was suggestive of a growth or survival defect in committed progenitor populations. Similar to $Fancc^{-/-}$ $Sod1^{-/-}$ mice, in vitro colony generation by FA BM samples was

Downloaded from http://ashpublications.net/blood/article-pdf/98/4/1003/1676353/h8160101003.pdf by guest on 05 June 2024

impaired at both the multipotential and differentiated progenitor levels,[48-50] with the mean CFU-GM values for human FA colony-forming cells being approximately 15-fold lower than controls.[50] In contrast to humans with *FANCC* mutations, however, *Fancc*$^{-/-}$ mice do not show spontaneous permanent cytopenias or decreased clonogenic potential.[13,14] Like their human counterparts, however, hematopoietic cells from *Fancc*$^{-/-}$ show increased sensitivity to interferon-γ, tumor necrosis factor-α, and macrophage inflammatory protein-1α, as well as deregulated apoptosis.[51] *Fancc*$^{-/-}$ BM cells also exhibit a decrease (7- to 12-fold) in short-term and long-term multilineage repopulating ability.[52] The mild thrombocytopenia we observed in young (8-10 week), but not older (3 month) *Fancc*$^{-/-}$ mice had not been reported previously, and is likely attributable to differences in the genetic backgrounds of the mice. This variable may also account for the modest reductions in myeloid and lymphoid colony formation in our *Fancc*$^{-/-}$ mice. Unlike individuals with FA, platelet counts of young *Fancc*$^{-/-}$*Sod1*$^{-/-}$ mice were normal. It is possible that thrombocytopenia would occur over time were BM failure progressive in these mice. Interestingly, increased MCV of *Fancc*$^{-/-}$*Sod1*$^{-/-}$ RBCs was analogous to the macrocytosis commonly observed in patients with FA[53]; however, this morphology has many causes, including liver dysfunction.[54]

The finding of impaired hematopoiesis in *Fancc*$^{-/-}$*Sod1*$^{-/-}$ mice was most strongly supported by our functional studies of in vitro growth of committed progenitors. CFU-GEMMs, CFU-GMs, and CFU-preBs from *Fancc*$^{-/-}$*Sod1* BM samples failed to grow. Furthermore, despite normal levels of the earliest (Lin^{-}) progenitors, there were considerably lower numbers of Lin^{+} progenitors/femur in *Fancc*$^{-/-}$*Sod1*$^{-/-}$ mice. In addition, the ability of BM cells to produce colonies of normal size and containing the usual range of cell types was compromised. In keeping with a markedly reduced proliferative potential (or an increased rate of apoptosis) CFU numbers in vitro were not increased by simply plating more cells (up to 10-fold). Thus, poor *Fancc*$^{-/-}$*Sod1*$^{-/-}$ colony formation did not appear to result from the plating of lower progenitor numbers, but instead pointed to a progenitor cell growth or survival defect. Although *Fancc*$^{-/-}$*Sod1*$^{-/-}$ total BM samples did not reveal evidence of overt apoptosis, increased death restricted to a progenitor subset(s) would readily explain the lack of growth in the *Fancc*$^{-/-}$*Sod1*$^{-/-}$ colony-forming assays. This might be attributable to superoxide-mediated genotoxicity superimposed on a background of reduced DNA repair capacity due to the lack of Fancc. Although oxygen-dependent toxicity did not appear to play a role in colony-forming assay inhibition (growth in 5% oxygen did not "rescue" growth), it is possible that committed progenitors have pro-oxidant intracellular environments that result in toxicity even at reduced oxygen tensions, or that marrow *Fancc*$^{-/-}$*Sod1*$^{-/-}$ progenitors were damaged by ambient oxygen during harvesting and initial colony-forming assay plating procedures.

Alternatively, because ROS appear to be required for the normal proliferative response to various growth factors,[55] it is possible that Sod1 deficiency led to loss of a positive growth signal. There is evidence that ROS, such as superoxide and hydrogen peroxide, can act as second messengers for a variety of stimuli, including growth factors.[55] GM-colony-stimulating factor stimulation, for example, led to rapid increases in cellular hydrogen peroxide levels, accompanied by elevated levels of tyrosine phosphorylation.[56] The latter may be due to the transient inhibition of protein-tyrosine phosphatases by this species, an event predicted to favor protein-tyrosine kinase-dependent signaling.[55] Furthermore, alterations in redox potential affect a wide range of cellular processes.[40,55] The balance between ROS and antioxidant systems may thus regulate cellular responses to external stimuli[40,56,57]; for example, interfering with hydrogen peroxide generation attenuated the proliferative response of hematopoietic cells to colony-stimulating factors. A lack of Sod1 would be predicted to inhibit growth factor–mediated cell growth by reducing conversion of superoxide to hydrogen peroxide. Thus, hematopoietic progenitors from *Fancc*$^{-/-}$*Sod1*$^{-/-}$ mice might be intrinsically hyporesponsive to growth factor stimulation. Perhaps in keeping with this, we observed a consistent reduction in colony formation in vitro when *Sod1*$^{-/-}$ BM samples were plated. It is also notable that the abnormalities of *Fancc*$^{-/-}$*Sod1*$^{-/-}$ mice are analogous to those of *W/Wv* mice that lack normal stem cell factor receptor kinase (c-kit) activity and demonstrate a marked suppression of CFU growth in vitro.[58] There is evidence that FANCC is required for normal STAT1 activation following growth factor stimulation.[59] This intriguing finding raises the possibility that a "2-hit" signaling abnormality might account for the hematopoietic defect of *Fancc*$^{-/-}$*Sod1*$^{-/-}$mice: namely, that a decreased level of growth factor-induced ROS (specifically, hydrogen peroxide), together with a defect in STAT1-mediated signaling, act synergistically to inhibit proliferation and/or survival of hematopoietic progenitors.

Acknowledgments

We are indebted to Dr R. K. Humphries of the Terry Fox Laboratory (Vancouver, BC) for his critical review of our data, and to S. Middler and J. Patterson of the British Columbia Children's and Women's Hospital Pathology Laboratory for preparing samples for electron microscopy and for the analysis of blood samples. We also thank L. Spence who performed the genotyping, S. Smith and T. McKernan in the Centre for Molecular Medicine and Therapeutics vivarium, and N. Makhani for her assistance.

References

1. Fanconi G. Familial constitutional panmyelocytopathy, Fanconi anemia (F.A.). Semin Hematol. 1967;4:233-240.
2. Scriver CR. The Metabolic and Molecular Bases of Inherited Disease, 7th ed. New York: McGraw-Hill; 1995.
3. Ishida R, Buchwald M. Susceptibility of Fanconi's anemia lymphoblasts to DNA-cross-linking and alkylating agents. Cancer Res. 1982;42:4000-4006.
4. Lo Ten Foe JR, Rooimans MA, Bosnoyan Collins L, et al. Expression cloning of a cDNA for the major Fanconi anaemia gene, FAA. Nat Genet. 1996;14:320-323.
5. Consortium FABC. Positional cloning of the Fanconi anemia group A gene. Nat Genet. 1996;14:324-328.
6. Strathdee CA, Gavish H, Shannon WR, Buchwald M. Cloning of cDNAs for Fanconi's anemia by functional complementation. Nature. 1992;356:763-767.
7. de Winter JP, Waisfisz Q, Rooimans MA, et al. The Fanconi anemia group G gene FANCG is identical with XRCC9. Nat Genet. 1998;20:281-283.
8. de Winter JP, Rooimans MA, van Der Weel L, et al. The Fanconi anaemia gene FANCF encodes a novel protein with homology to ROM. Nat Genet. 2000;24:15-16.
9. de Winter JP, Leveille F, van Berkel CG, et al. Isolation of a cDNA representing the Fanconi anemia complementation group E gene. Am J Hum Genet. 2000;67:1306-1308.
10. Timmers C, Taniguchi T, Hejna J, et al. Positional cloning of a novel Fanconi anemia gene, FANCD2. Mol Cell. 2001;7:241-248.
11. Buchwald M. Complementation groups: one or more per gene? Nat Genet. 1995;11:228-230.
12. Wevrick R, Clarke CA, Buchwald M. Cloning and analysis of the murine Fanconi anemia group C cDNA. Hum Mol Genet. 1993;2:655-662.
13. Whitney MA, Royle G, Low MJ, et al. Germ cell defects and hematopoietic hypersensitivity to gamma-interferon in mice with targeted disruption

Downloaded from http://ashpublications.net/blood/article-pdf/98/4/1003/1676353/h8160101003.pdf by guest on 05 June 2024

of the Fanconi anemia C gene. Blood. 1996;88: 49-58.

14. Chen M, Tomkins DJ, Auerbach W, et al. Inactivation of Fac in mice produces inducible chromosomal instability and reduced fertility reminiscent of Fanconi anaemia. Nat Genet. 1996;12:448-451.
15. Buchwald M, Moustacchi E. Is Fanconi anemia caused by a defect in the processing of DNA damage? Mutat Res. 1998;408:75-90.
16. Pagano G. Mitomycin C and diepoxybutane action mechanisms and FANCC protein functions: further insights into the role for oxidative stress in Fanconi's anaemia phenotype. Carcinogenesis. 2000;21:1067-1068.
17. Ruppitsch W, MeiBlitzer C, Hirsch Kauffmann M, Schweiger M. Overexpression of thioredoxin in Fanconi anemia fibroblasts prevents the cytotoxic and DNA damaging effect of mitomycin C and diepoxybutane. FEBS Lett. 1998;422:99-102.
18. Schindler D, Hoehn H. Fanconi anemia mutation causes cellular susceptibility to ambient oxygen. Am J Hum Genet. 1988;43:429-435.
19. Joenje H, Arwert F, Eriksson AW, de Koning H, Oostra AB. Oxygen-dependence of chromosomal aberrations in Fanconi's anaemia. Nature. 1981; 290:142-143.
20. Kubbies M, Schindler D, Hoehn H, Schinzel A, Rabinovitch PS. Endogenous blockage and delay of the chromosome cycle despite normal recruitment and growth phase explain poor proliferation and frequent edomitosis in Fanconi anemia cells. Am J Hum Genet. 1985;37:1022-1030.
21. Korkina LG, Samochatova EV, Maschan AA, et al. Release of active oxygen radicals by leukocytes of Fanconi anemia patients. J Leukoc Biol. 1992;52:357-362.
22. Degan P, Bonassi S, de caterina M, et al. In vivo accumulation of 8-hydroxy-2′-deoxyguanosine in DNA correlates with release of reactive oxygen species in Fanconi's anemia families. Carcinogenesis. 1995;16:735-742.
23. Ruppitsch W, Meiblitzer C, Weirich Schwaiger H, et al. The role of oxygen metabolism for the pathological phenotype of Fanconi anemia. Hum Genet. 1997;99:710-719.
24. Kruyt FAE, Hoshino T, Liu JM, et al. Abnormal microsomal detoxification implicated in Fanconi anemia group C by interaction of the FAC protein with NADPH cytochrome P450 reductase. Blood. 1998;92:3050-3056.
25. Shefner JM, Reaume AG, Flood DG, et al. Mice lacking cytosolic copper/zinc superoxide dismutase display a distinctive motor axonopathy. Neurology. 1999;53:1239-1246.
26. Flood DG, Reaume AG, Gruner JA, et al. Hindlimb motor neurons require Cu/Zn superoxide dismutase for maintenance of neuromuscular junctions. Am J Pathol. 1999;155:663-672.
27. Ho Y, Gargano M, Cao J, et al. Reduced fertility in female mice lacking copper-ainc superoxide dismutase. J Biol Chem. 1998;273:7765-7769.
28. Reaume AG, Elliott JL, Hoffman EK, et al. Motor neurons in Cu/Zn superoxide dismutase-deficient mice develop normally but exhibit enhanced cell death after axonal injury. Nat Genet. 1996;13:43-47.
29. Kondo T, Reaume AG, Huang TT, et al. Reduction of CuZn-superoxide dismutase activity exacerbates neuronal cell injury and edema formation after transient focal cerebral ischemia. J Neurosci. 1997;17:4180-4189.
30. Huang TT, Yasunami M, Carlson EJ, et al. Superoxide-mediated cytotoxicity in superoxide dismutase-deficient fetal fibroblasts. Arch Biochem Biophys. 1997;344:424-432.
31. Applegate LA, Luscher P, Tyrrell RM. Induction of heme oxygenase: a general response to oxidant stress in cultured mammalian cells. Cancer Res. 1991;51:974-978.
32. Otterbein LE, Kolls JK, Mantell LL, et al. Exogenous administration of heme oxygenase-1 by gene transfer provides protection against hyperoxia-induced lung injury. J Clin Invest. 1999;103: 1047-1054.
33. Yeh CC, Wan XS, St Clair DK. Transcriptional regulation of the 5′ proximal promoter of the human manganese superoxide dismutase gene. DNA Cell Biol. 1998;17:921-930.
34. Williams MD, Van Remmen H, Conrad CC, et al. Increased oxidative damage is correlated to altered mitochondrial function in heterozygous manganese superoxide dismutase knockout mice. J Biol Chem. 1998;273:28510-28515.
35. Doull CA. Toxicology: The Basic Science of Poisons. 5th ed. New York: McGraw-Hill; 1996.
36. Hancock JT. Superoxide, hydrogen peroxide and nitric oxide as signalling molecules; their production and role in disease. Br J Biomed Sci. 1997; 54:38-46.
37. Jaeschke H. Mechanisms of oxidant stress-induced acute tissue injury. Drug Metab Reviews. 1995;209:104-111.
38. Toyokuni S. Reactive oxygen species-induced molecular damage and its application in pathology. Pathol Int. 1999;49:91-102.
39. Lebovitz RM, Zhang H, Vogel H, et al. Neurodegeneration, myocardial injury, and perinatal death in mitochondrial superoxide dismutase-deficient mice. Proc Natl Acad Sci U A A. 1996;93:9782-9787.
40. Finkel T. Oxygen radicals and signaling. Curr Opin Cell Biol. 1998;10:248-253.
41. Dalton TP, Shertzer HG, Puga A. Regulation of gene expression by reactive oxygen. Annu Rev Pharmacol Toxicol. 1999;39:67-101.
42. Nordenson I. Effect of superoxide dismutase and catalase on spontaneously occurring chromosomal breaks in patients with Fanconi's anemia. Hereditas. 1977;86:147-150.
43. Nagasawa H, Little JB. Suppression of cytotoxic effect of mitomycin-C by superoxide dismutase in Fanconi's anemia and dyskeratosis congenita fibroblasts. Carcinogenesis. 1983;4:795-798.
44. Joenje H, Eriksson AW, Frants RR, Arwert F, Houwen B. Erythrocyte superoxide-dismutase deficiency in Fanconi's anaemia. Lancet. 1978;1:204.
45. Okahata S, Kobayashi Y, Usui T. Erythrocyte superoxide dismutase activity in Fanconi's anaemia. Clin Sci (Colch). 1980;58:173-175.
46. Mavelli I, Ciriolo MR, Rotilio G, et al. Superoxide dismutase, glutathione peroxidase and catalase in oxidative hemolysis. A study of Fanconi's anemia erythrocytes. Biochem Biophys Res Commun. 1982;106:286-290.
47. Hautekeete ML, Degott C, Benhamou JP: Microvesicular steatosis of the liver. Acta Clin Belg. 1990;45: 311-326.
48. Alter BP, Knobloch ME, Weinberg RS. Erythropoiesis in Fanconi's anemia. Blood. 1991;78:602-608.
49. Bagnara GP, Strippoli P, Bonsi L, et al. Effect of stem cell factor on colony growth from acquired and constitutional (Fanconi) aplastic anemia. Blood. 1992;80:382-387.
50. Stark R, Thierry D, Richard P, Gluckman E. Long-term bone marrow culture in Fanconi's anemia. Br J Haematol. 1993;83:554-559.
51. Haneline LS, Broxmeyer HE, Cooper S, et al. Multiple inhibitory cytokines induce deregulated progeitor growth and apoptosis in hematopoietic cells from Fac−/− mice. Blood. 1998;91:4092-4098.
52. Haneline LS, Gobbett TA, Ramani R, et al. Loss of FancC function results in decreased hematopoietic stem cell repopulating ability. Blood. 1999; 94:1-8.
53. D'Andrea AD, Grompe M: Molecular biology of Fanconi anemia: implications for diagnosis and therapy. Blood. 1997;90:1725-1736.
54. Nathan DG, Orkin SH. Hematology of Infancy and Childhood, vol 2. 5th ed. Philadelphia: Saunders; 1998.
55. Rhee SG, Bae YS, Lee S, Kwon J. Hydrogen peroxide: a key messenger that modulates protein phosphorylation through cystein oxidation. Science. 2000;53:1-6.
56. Sattler M, Winkler T, Verma S, et al. Hematopoietic growth factors signal through the formation of reactive oxygen species. Blood. 1999;93:2928-2935.
57. McCord JM, Fridovich I. The biology and pathology of oxygen radicals. Annals of Int Medicine. 1978; 89:122-127.
58. Tyler WS, Stohlman F Jr, Chovaniec M, Howard D. Effect of a congenital defect in hemopoiesis on myeloid growth and the stem cell (CFU) in an in vivo culture system. Blood. 1976;47:413-421.
59. Pang Q, Fagerlie S, Christianson TA, et al. The Fanconi anemia protein FANCC binds to and facilitates the activation of STAT1 by gamma interferon and hematopoietic growth factors. Mol Cell Biol. 2000;20:4724-4735.

Downloaded from http://ashpublications.net/blood/article-pdf/98/4/1003/1676353/h8160101003.pdf by guest on 05 June 2024